γ-band staggering and E(5)-type structure: ^{64}Zn

C. Mihai, N. V. Zamfir, D. Bucurescu, G. Căta-Danil,* I. Căta-Danil, D. G. Ghiţă, M. Ivaşcu, T. Sava, L. Stroe, and G. Suliman

National Institute of Physics and Nuclear Engineering, Bucharest-Măgurele, Romania

(Received 4 October 2006; revised manuscript received 29 January 2007; published 6 April 2007)

The staggering factor S_4 in the quasi-γ band was used for the first time as a signature of the E(5) symmetry. This observable, together with the $R_{4/2}$ ratio is used to find E(5) type nuclei in the $Z = 28$–50 and $Z = 50$–82 shells. An E(5) candidate is found to be ^{64}Zn. Low-spin states in ^{64}Zn populated in the ϵ/β^+ decay of ^{64}Ga, produced in the ^{54}Fe(^{12}C,*pn*)^{64}Ga, were studied through off-beam γ-ray spectroscopy. The decay scheme of ^{64}Zn is found to be reasonably close to the predictions of the E(5) critical point symmetry. The structure of the excited 0^+ states in ^{64}Zn and their behavior in the Zn isotopic chain is discussed.

DOI: 10.1103/PhysRevC.75.044302 PACS number(s): 27.50.+e, 21.60.Ev, 21.60.Fw, 23.20.Lv

I. INTRODUCTION

Nuclear collectivity is often described in the context of three benchmark models: the spherical vibrator [1], the axial symmetric rotor [2] and the γ-soft model [3]. These are idealized limits codified in the framework of the interacting boson approximation (IBA) model [4] in terms of the U(5), SU(3) and O(6) dynamical symmetries, respectively. It was shown in refs. [5,6] in the framework of the IBA model, using the intrinsic state formalism [7], that there are shape/phase transitions in the evolution of nuclear shapes from spherical to deformed. Using the Bohr Hamiltonian with flat-bottomed potentials in the quadrupole deformation, Iachello introduced new dynamical symmetries at the critical point of these transitions: E(5) for a transition between spherical and γ-soft deformed nuclei [8] and X(5) for a transition between spherical and axially symmetric deformed nuclei [9]. Empirical evidence of such transitions was found in many nuclei situated in transitional mass regions [10–14].

The most basic structural signature of the E(5) symmetry is a value of the ratio $R_{4/2} = E_{4_1^+}/E_{2_1^+}$ of 2.20. This value is intermediate between the values for spherical nuclei (2.00) and γ-soft structure (2.50), but also intermediate between the values for spherical nuclei and axial symmetric quadrupole deformed (3.33). Thus, an interpretation based only on the $R_{4/2}$ ratio can be ambigous and additional signatures need to be considered. Often, the decay properties of the lowest excited 0^+ states are used as an additional signature of the E(5) structure. The branching ratios of the transitions deexciting the lowest excited 0^+ states are also, sometimes, ambiguous being very similar in the entire transition region between spherical and deformed γ-soft nuclei [O(5) type structure]. The absolute transition strengths are needed to be considered, but they are difficult to measure and often, this information is unavailable.

Here, we propose as an additional signature for identifying empirical E(5) candidates, the quasi-γ band staggering index, S_4, related to the γ degree of freedom [15].

*Permanent address: Physics Department, University Politehnica of Bucharest, Romania.

We performed a survey of the $Z = 28$–50 and $Z = 50$–82 shells, using both the $R_{4/2}$ and S_4 parameters as indicators for possible E(5) structure. We identified those nuclei having these properties close to an E(5) type structure. For the first time, we propose a few possible candidates in the $Z, N = 28$–50 shell. The only one with known lifetimes for the excited 0^+ states is ^{64}Zn, but the data on the corresponding branching ratios is controversial.

Low-lying nonyrast states in ^{64}Zn, which are relevant for a comparison with E(5) predictions, were previously populated by various methods [16], one of the most complete set of data being obtained from ϵ/β^+ decay of ^{64}Ga experiments. Unfortunately, as in many other cases on the nuclide chart, these experiments were performed 30–40 years ago, with NaI(Tl) or small Ge(Li) γ-ray detectors, even with no coincidence measurements [17–19]. Very often, in order to have a reliable set of data it is necessary to perform new measurements of γ-ray intensities in high resolution γ-γ experiments. In the work reported in the present paper we measured for the first time the intensities of the γ rays in ^{64}Zn following the ϵ/β^+ decay of ^{64}Ga through γ-γ coincidences using high resolution Ge detectors. We interpret the results, including the properties of the first two excited 0^+ states, using the E(5) symmetry as a benchmark.

II. SEARCH FOR E(5) TYPE NUCLEI

As mentioned in the Introduction, we have performed an extensive search over a wide mass region ($Z = 28$–82, $N = 28$–104) in order to find the most suitable candidates for the E(5) symmetry. The E(5) symmetry describes nuclei that are at the critical point of the transition from a spherical shape to a γ-soft deformed shape. In order to find the E(5) candidates we studied how collectivity evolves in this mass region. An important signature of the quadrupole collectivity is the ratio $R_{4/2} = E_{4_1^+}/E_{2_1^+}$. The value of this ratio in E(5) is 2.20, intermediate between a spherical vibrator or U(5) ($R_{4/2} = 2.00$) and the γ-soft model or O(6) ($R_{4/2} = 2.50$).

We also took under consideration in our analysis the staggering factor S_4 [15], a quantitative measure of the γ

 ©2007 The American Physical Society

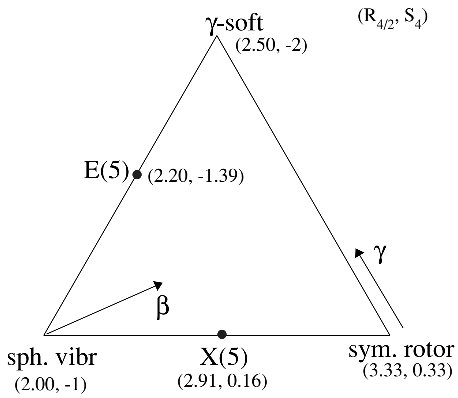

FIG. 1. Casten's symmetry triangle in its geometric representation with the critical point symmetries E(5) and X(5).

softness, defined as

$$S_4 = \frac{(E_{4^+_\gamma} - E_{3^+_\gamma}) - (E_{3^+_\gamma} - E_{2^+_\gamma})}{E_{2^+_g}}, \qquad (1)$$

where the γ subscript referes to levels from the quasi-γ band. The S_4 factor is a measure of the dependence of the geometric Hamiltonian on the γ coordinate. For the E(5) dynamical symmetry the staggering factor also takes an intermediate value ($S_4 = -1.39$) between the spherical vibrator ($S_4 = -1$) and the γ-soft model ($S_4 = -2$).

The ENSDF data base [20] was used to calculate the $R_{4/2}$ and S_4 parameters for nuclei with $Z = 28$–82 and $N = 28$–104. In the cases where no definite assignment for the quasi-γ band was given, we considered the levels 4^+_2, 2^+_2, and 3^+_1 as the 4^+_γ, 2^+_γ, and 3^+_γ, respectively.

Figure 1 shows Casten's symmetry triangle [21] in its geometric representation with the critical point symmetries E(5) and X(5). Each vertex represents a geometric limit and the legs denote regions where the structure undergoes a transition from one limit/shape to another. The $R_{4/2}$ and S_4 parameters are specified for each geometric limit and critical point.

The use of both $R_{4/2}$ and S_4 parameters as signatures of collectivity, gives information about both basic geometric degrees of freedom, the quadrupole deformation and the γ softness, practically indicating the position of a given nucleus in Casten's symmetry triangle [21].

Figures 2, 3, 4, 5 shows the $R_{4/2}$ ratio and the S_4 staggering index for nuclei in the $Z, N = 28$–50 shell, $Z = 28$–50, $N = 50$–82 shell, $Z, N = 50$–82 shell and $Z = 50$–82 shell, $N = 82$–104 half shell, respectively. The values highlighted in bold face characters correspond to values of the $R_{4/2}$ ratio close the prediction of the E(5) symmetry of 2.20 or to values of the S_4 factor close to the E(5) predictions of -1.39. The nuclei with both the $R_{4/2}$ and S_4 values closest to those predicted by the E(5) symmetry are a) for the $Z, N = 28$–50 shell (Fig. 2) ^{64}Zn, ^{68}Zn, and ^{64}Ge; b) for $Z = 28$–50, $N - 50$–82 shell (Fig. 3) ^{112}Cd, ^{114}Cd, ^{100}Pd, and ^{102}Pd; c) for the $Z, N = 28$–50 shell (Fig. 4) ^{136}Ba; d) for the $Z = 50$–82 shell, $N = 82$–104 half shell (Fig. 5) ^{146}Nd, ^{148}Sm, and ^{150}Sm. Two of these nuclei were previously proposed as good E(5) nuclei: ^{102}Pd ([11]) and ^{114}Cd ([14]).

In the $Z, N = 28$–50 shell, the evolution of collectivity is not very clear despite the monotonic behavior of the $R_{4/2}$ and S_4 parameters. This shell is not wide enough to show a full transition between two symmetries.

It is worth mentioning that this type of analysis reveals also the best candidates for X(5)-type structure. The nuclei with the $R_{4/2}$ and S_4 values close to the prediction of the X(5) symmetry ($R_{4/2} = 2.91$, $S_4 = 0.16$ [22]) in the $Z = 50$–82 shell, $N = 82$–104 half shell are the $N = 90$ isotopes of Nd, Sm, Gd, and Dy, ^{162}Yb, ^{166}Hf, ^{170}W, and ^{176,178}Os. These nuclei were already considered as X(5) candidates (for a review see [23]).

We investigate here the structure of ^{64}Zn which seems to be close to the E(5) predictions.

50 Sn	**$R_{4/2}$** **S_4**											
48 Cd											-	
46 Pd									- -	- -	**(2.11)** **-**	
44 Ru								- -	**(2.29)** **-**	**(2.24)** **-**	**(2.14)** **-**	
42 Mo								- -	(2.34) -	**2.23** **-**	**2.11** **-**	
40 Zr						- -	(2.85) -	2.56 -	2.34 -0.26	**2.22** (-0.42)	2.02 -	
38 Sr					- -	- -	(2.81) -	2.54 (-0.43)	2.32 -0.35	**2.23** (-0.07)	2.07 -	
36 Kr				- -	(1.86) -	**2.22** **-**	2.44 (-0.68)	2.46 (-0.72)	2.33 -0.28	2.34 (-0.37)	2.38 -	
34 Se			- -	**(2.27)** -	**2.16** **-**	1.90 -	**2.15** -0.61	2.38 -0.24	2.45 0.34	2.55 0.45	2.65 0.40	
32 Ge		- -	**(2.27)** **(-1.78)**	**2.27** (-0.59)	**2.23** -0.24	2.07 -0.37	2.07 -0.73	2.46 (0.12)	2.51 (0.08)	2.54 (0.3)	(2.64) -	
30 Zn		**2.18** **-**	**2.29** -0.23	**2.33** **-1.66**	2.36 (-0.74)	**(2.24)** **(-1.09)**	2.02 **(-1.63)**	- -	(1.92) -	(2.16) -	- -	
28 Ni												
Z ╲ N	28	30	32	34	36	38	40	42	44	46	48	50

FIG. 2. The $R_{4/2}$ and S_4 parameters (see text) in the $Z, N = 28, 50$ shell. The values close to the E(5) prediction of 2.2 ($\pm$0.1) for the $R_{4/2}$ parameter and -1.39 ($|S_4| > 1$) for the staggering index are highlighted in bold face characters. The ENSDF data base [20] was used to calculate the $R_{4/2}$ and S_4 parameters.

Z \ N	50	52	54	56	58	60	62	64	66
50 Sn	**$R_{4/2}$** **S_4**								
48 Cd		1.79 -	**2.11** -	**2.26** -	2.36 (-1.09)	2.38 -4.25	2.34 5.62	**2.29** **-1.53**	**2.3** **(-1.41)**
46 Pd		1.78 -	**2.12** **(-1.91)**	**2.29** **-0.99**	2.38 -0.39	2.40 (-0.11)	2.41 (-0.26)	2.46 (-0.57)	(2.53) -
44 Ru		1.82 (-0.79)	**2.14** -0.18	**2.27** (-0.63)	2.32 (-0.71)	2.48 -	2.64 -	2.74 (-0.24)	2.75 (-0.09)
42 Mo		1.80 **(-1.67)**	2.09 -0.76	1.91 (-2.52)	**2.12** (-0.71)	2.51 -0.82	2.91 -0.15	3.04 -	2.92 -0.01
40 Zr		1.60 **-1.68**	1.60 **-1.10**	1.57 (0.12)	(1.50) -	(2.65) -	- -	3.22	- -

FIG. 3. Similar to Fig. 2 but for the $Z = 28$–50, $N = 50$–82 shell.

III. THE CASE OF ^{64}ZN: EXPERIMENT AND DISCUSSION

The low-lying nonyrast states of ^{64}Zn were populated in the ϵ/β^+ decay of the 0^+ ($T_{1/2} = 157.6$ s) ground state of ^{64}Ga and studied offline through γ-ray spectroscopy. The parent nuclei were produced through the ^{54}Fe(^{12}C,pn)^{64}Ga reaction. A self-supported 13 mg/cm^2 99% enriched in ^{54}Fe target was bombarded with a 3 pnA, 36 MeV ^{12}C beam provided by the Bucharest FN Tandem. The statistical model code CASCADE [24] was used to evaluate the population cross sections of the reaction. The strongest channels were estimated to be the following (the cross sections are normalized to the fusion cross section): $2p$ (^{64}Zn, stable) with a cross section of 35%, pn (^{64}Ga, $T_{1/2} = 157.6$ s) with 25%, $2pn$ (^{63}Zn, $T_{1/2} = 38.5$ min.) with 10% and $p\alpha$(^{61}Cu, $T_{1/2} = 3.3$ h) with 15%.

In order to optimize the production rate of ^{64}Ga, the beam was chopped with a period of 250 s. To assure clean γ-ray spectra without contamination from prompt transitions, the chopper system started the data acquisition 12 ms after switching off the beam.

The γ-rays were detected using an array of three HPGe detectors with efficiency around 25%. Both γ-ray singles and γ-γ coincidences were simultaneously recorded in event mode. A singles spectrum is shown in Fig. 6 (top) and a γ-γ coincidence data gated on the 991 keV $2_1^+ \to 0_1^+$ transition is shown in Fig. 6 (bottom). The energy range of the spectrum was limited to $E_\gamma^{max} \approx 3.7$ MeV. The singles spectrum shows contamination with background lines and transitions from other reaction channels (especially the $p\alpha$ and $2pn$ channels) with relatively small intensities, while the coincidence data are extremely clean, as shown in Fig. 6.

Table I summarizes the γ-rays observed in this experiment and assigned to ^{64}Zn based on the γ-γ coincidences, including their placements and intensities. The results confirm in general the data presented in Ref. [16] with a few exceptions that are marked in Table I. We were interested in reevaluating the decay properties of the low-lying states, especially of the first two excited 0^+ states and we will discuss them in detail.

(i) The 0_2^+ state at 1910 keV. A 110 keV transition to the 2_2^+ state with a relative intensity ($I_{991} = 100$) of 0.50(5) was reported by Refs. [25,26], in (p, $p\prime\gamma$) and electron conversion studies. This transition was not reported in any γ-γ study [16]. From the coincidence data, a relative intensity of 0.59(19) for the 110 keV transition was measured, which is in agreement with the result of Refs. [25,26]. The state also decays to the 2_1^+ state through a 918 keV transition with an intensity of 18.7(4) [16]. The measured intensity for the 918 keV transition is also in agreement with previous studies. Considering the measured lifetime [16], the transition strengths are $B(E2{:}0_2^+ \to 2_2^+) = 60(8)$ W.u. for the 110 keV transition and $B(E2{:}0_2^+ \to 2_1^+) = 0.058(3)$ W.u. for the 918 keV transition.

(ii) The 0_3^+ state at 2609 keV. A 809 keV transition deexciting the 2609 keV state to the 2_2^+ state at 1799 keV was

Z \ N	58	60	62	64	66	68	70	72	74	76	78	80	82
68 Er	**$R_{4/2}$** **S_4**											(2.35) -	
66 Dy									(2.80) -	(2.53) -	(2.37) -	(2.35) -	
64 Gd									2.74 -	2.54 (-0.43)	2.35 -	(2.35) -	
62 Sm							(3.18) -	2.94 -	2.69 -	2.57 (-0.07)	2.34 -	2.33 -	
60 Nd						(3.17) -	3.05 -	2.87 (-1.83)	2.68 (-0.38)	2.61 (-0.15)	2.40 (-0.09)	2.33 -	
58 Ce					(3.15) -	3.06 (-0.11)	2.92 -0.46	2.80 (-0.78)	2.64 -0.59	2.56 -0.38	2.37 -	2.32 (-0.90)	
56 Ba			(2.86) -	(2.92) -	(2.91) -	2.83 (-0.85)	2.78 -0.99	2.69 -1.38	2.52 (-0.94)	2.42 -0.56	2.32 -0.25	**2.28** **-1.54**	
54 Xe		2.38 -	2.33 (-0.95)	2.40 **(-1.07)**	2.46 -0.82	2.50 (-0.55)	2.48 -0.59	2.42 -0.69	2.33 -0.65	**2.25** (-0.62)	**2.16** -0.52	2.04 -	
52 Te	**2.13** -	**2.14** -	2.09 (-0.68)	2.00 -0.46	1.99 **(-1.53)**	2.07 **-1.27**	2.09 -	2.07 -2.79	2.04 **-1.24**	2.01 **-1.05**	1.94 -	1.72 -	
50 Sn													

FIG. 4. Similar to Fig. 2 but for the Z, $N = 50$–82 shell.

82 Pb	**$R_{4/2}$** **S_4**										
80 Hg							2.23 -		1.63 -	1.74 -	1.78 -
78 Pt				**2.30** -		**2.26** -	**2.13** -	(2.51) -	2.68 **(-1.29)**	2.70 **(-1.19)**	2.67 **(-1.08)**
76 Os			**(2.20)** -			2.62 -	2.66 (0.18)	2.74 -0.04	2.92 0.10	3.02 0.10	3.09 0.16
74 W	- -	2.07 -	- -	2.48 -	2.68 -	2.82 -	2.95 (0.06)	3.06 -	3.15 -	3.21 (0.03)	3.24 -
72 Hf	(1.85) -	(2.17) -	2.31 -	2.56 -	2.79 -	2.97 (0.07)	3.11 (0.25)	3.19 (0.13)	3.25 (0.19)	3.27 (0.03)	3.28 (-0.11)
70 Yb	(1.84) -	**2.13** -	2.33 -	2.62 -	2.92 (-0.01)	3.13 (0.01)	3.23 0.17	3.27 (0.24)	3.29 (0.29)	3.31 0.32	3.31 (0.27)
68 Er	1.83 -	2.07 -	**2.31** (-0.59)	2.74 -0.43	3.10 (0.07)	3.23 0.24	3.28 0.28	3.29 0.29	3.31 0.30	3.31 (0.51)	3.31 -
66 Dy	1.81 -	2.05 -	**2.23** -0.59	2.93 0.11	3.20 0.21	3.27 0.27	3.29 0.29	3.30 0.29	(3.31) (0.30)	(3.31) -	
64 Gd	1.80 -	2.02 -	**2.19** -0.61	3.01 0.04	3.24 0.15	3.29 0.18	3.30 0.28	3.29 (0.26)	(3.30)		
62 Sm	1.84 -	**2.14** **-1.12**	**2.31** **-1.54**	3.01 (-0.08)	3.25 0.32	3.29 -	(3.30) -	3.29 -			
60 Nd	1.89 -	**2.29** **-1.12**	2.49 -0.82	2.92 (0.11)	3.26 -	3.29 -	3.32 -				
58 Ce	1.90 -	2.36 (-0.55)	2.59 (-0.98)	(2.86) (-0.47)	(3.15) -	(3.23) -					
56 Ba	1.87 -	2.32 -	2.66 -	2.83 -	2.98 -						
54 Xe	1.82 -	**2.21** -	2.40 -	(2.55) -							
52 Te	1.70 -	(2.04) -									
50 Sn											
Z / N	82	84	86	88	90	92	94	96	98	100	102	104

FIG. 5. Similar to Fig. 2 but for the $Z = 50$–82 shell, $N = 82$–104 half shell.

reported by Ref. [27], with a upper limit of 0.5% for the branching ratio $I_{809}/(I_{809} + I_{1618})$. We found no evidence for a 809 keV transition to the 2_2^+ level within our detection limit. The state decays also to the 2_1^+ state through a 1618 keV transition with an intensity of 3.81(19) [16]. The measured intensity of the 1618 keV transition is in good agreement with the value from Ref. [16]. From the measured lifetime [16] a $B(E2{:}0_3^+ \rightarrow 2_1^+) = 17(7)$ W.u. was extracted, and for the $B(E2{:}0_3^+ \rightarrow 2_2^+)$ an upper limit of 6 W.u. and a lower limit of 1.5 W.u. were estimated.

Figure 7 compares the experimental low-lying level scheme and transition strengths of ^{64}Zn with the predictions of the E(5) symmetry [8,28], scaled to the energy of the 2_1^+ state and $B(E2{:}2_1^+ \rightarrow 0_1^+)$ in ^{64}Zn. The experimental level energies and the transition strengths are as given in Ref. [16]. The two 3^+ states at 2979.79 keV and 3369.82 keV in ^{64}Zn are not collective according to the B(E2) values of their decay, the best candidate for the 3_γ^+ state was found to be the $(3)^+$ state at 3094 keV.

The E(5) symmetry seems to reproduce rather well the experimental data with a few important exceptions. The

TABLE I. γ-rays assigned to ^{64}Zn. Intensities are obtained from singles data or/and γ-γ coincidences and are normalized to 100 for the 991 keV $2_1^+ \rightarrow 0_1^+$ transition.

E_γ [a](keV)	E_{x_i}-E_{x_f} [b]	$J_i \rightarrow J_f$ [b]	I_{rel}
110.7[c]	1910-1799	$0_2^+ \rightarrow 2_2^+$	0.59(19)
577.3[d]	3186-2609	$1^+ \rightarrow 0_3^+$	0.21(4)
756.6	3366-2609	$1^+ \rightarrow 0_3^+$	2.77(19)
808.0	1799-991	$2_2^+ \rightarrow 2_1^+$	30.7(18)[e]
918.9	1910-991	$0_2^+ \rightarrow 2_1^+$	17.4(11)
991.6	991-0	$2_1^+ \rightarrow 0_1^+$	100
1185.4	3795-1910	$1^+ \rightarrow 0_2^+$	<0.16[f]
1276.4	3186-1910	$1^+ \rightarrow 0_2^+$	13.5(10)
1387.4	3186-1799	$1^+ \rightarrow 2_2^+$	26.5(23)
1455.9	3365-1910	$1^+ \rightarrow 0_2^+$	4.5(3)
1461.3	3262-1799	$1 \rightarrow 2_2^+$	<0.21[f]
1514.7	3425-1910	$1^+ \rightarrow 0_2^+$	0.51(8)[f]
1566.7	3365-1799	$1^+ \rightarrow 2_2^+$	4.65(36)[e]
1618.0	2609-991	$0_3^+ \rightarrow 2_1^+$	3.72(25)
1626.0	3425-1799	$1^+ \rightarrow 2_2^+$	2.49(17)
1799.7	1799-0	$2_2^+ \rightarrow 0_1^+$	9.11(64)[e]
1996.0	3795-1799	$1^+ \rightarrow 2_2^+$	3.93(34)[e]
2103.6	4712-2609	$(1) \rightarrow 0_3^+$	0.35(9)
2195.1	3186-991	$1^+ \rightarrow 2_1^+$	21.9(21)
2270.2	3262-991	$1 \rightarrow 2_1^+$	4.87(54)
2374.2	3365-991	$1^+ \rightarrow 2_1^+$	16.2(14)
2433.6	3425-991	$1^+ \rightarrow 2_1^+$	1.26(12)
2544.4	4454-1910	$1^+ \rightarrow 0_2^+$	0.30(6)
2655.2	4454-1799	$1^+ \rightarrow 2_2^+$	0.51(7)
2803.1	3795-991	$1^+ \rightarrow 2_1^+$	1.51(19)[e]
3186.8	3186-0	$1^+ \rightarrow 0_1^+$	0.47(8)
3261.7	3262-0	$1 \rightarrow 0_1^+$	0.31(2)
3365.3	3365-0	$1^+ \rightarrow 0_1^+$	31.5(34)
3424.8	3425-0	$1^+ \rightarrow 0_1^+$	10.1(10)
3617.1	4608-991	$(1) \rightarrow 2_1^+$	0.21(4)

[a]The error bars are estimated to be ≈ 0.1 keV for $E_\gamma <$ 1500 keV and ≈ 0.2 keV for $E_\gamma >$ 1500 keV.
[b]The energy and spin of the levels are as given in Ref. [16].
[c]New γ transition in ϵ/β^+ decay.
[d]New γ transition.
[e]Previously conflicting results.
[f]New intensity significantly different from previous data.

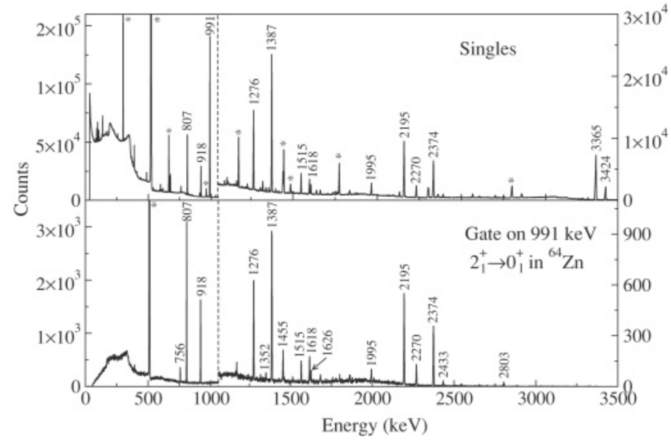

FIG. 6. Examples of off-beam γ-ray spectra following the reaction ^{12}C (36 MeV) $+^{54}$Fe. γ-rays assigned to ^{64}Zn are marked by their energies both in the singles and gated spectrum. Contaminant and background lines are marked with an asterisk.

multiphonon multiplet structure in ^{64}Zn presents high anharmonicities relative to the O(5) structure characteristic of the U(5)-O(6) leg of the symmetry triangle, which is also valid for the E(5) symmetry. The ground state band in ^{64}Zn is slightly more expanded in energy than the E(5) predictions. Figure 8 (left) compares the experimental level energies in the ground state band in ^{64}Zn with the predictions of the spherical vibrator, the γ-soft model and the E(5) symmetry normalized to the energy of the 2^+ state. The comparison shows that indeed ^{64}Zn lies close to the E(5) symmetry, slightly towards the γ-soft limit.

The transition strengths in the ground state band show also deviations from the E(5) predictions. Figure 8 (center) compares the experimental transition strengths in the ground state band of ^{64}Zn with the predictions of the spherical vibrator, γ-soft and E(5) geometric models. In the following, we make a special note about the experimental $B(E2{:}4_1^+ \rightarrow 2_1^+)$ value. In a recent paper [29] the lifetime of the 4_1^+ state at 2306 keV was remeasured. The surprising result emerging from this study: a $B(E2{:}4_1^+ \rightarrow 2_1^+) = 12(2)$ W.u., significantly smaller than $B(E2{:}2_1^+ \rightarrow 0_1^+) = 21.6(5)$ W.u., denoting a less collective structure of the 4_1^+ state. This less collective behavior of the 4_1^+ state was observed for other nuclei and is not yet explained [30]. Since some of this anomalous transition strengths highlighted in [30] were remeasured and dismissed [31], the newly measured anomalous transition strength $B(E2{:}4_1^+ \rightarrow 2_1^+)$ in ^{64}Zn also needs to be confirmed. In the present discussion we considered the value given in Ref. [16], which is more collective, as one would expect for a nucleus with eight nucleons over the closed shell.

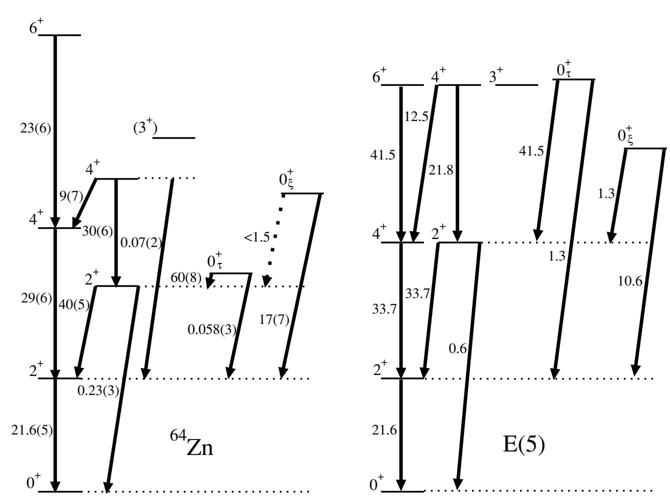

FIG. 7. Comparison between the experimental decay scheme of ^{64}Zn (left) and the predictions of the E(5) symmetry [28] (right) scaled to the energy of the 2_1^+ state and $B(E2{:}2_1^+ \rightarrow 0_1^+)$ in ^{64}Zn. Transitions are labeled by their transition strengths in W.u.

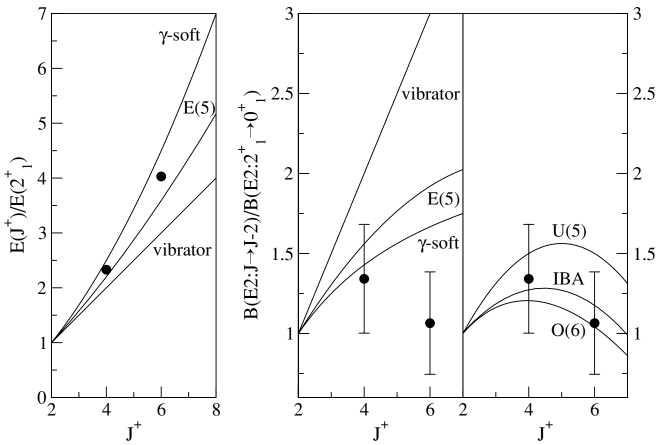

FIG. 8. Comparison between the relative experimental level energies (left) and relative transition strengths (center and right) in the ground state band of ^{64}Zn and the predictions of the geometric models and IBA.

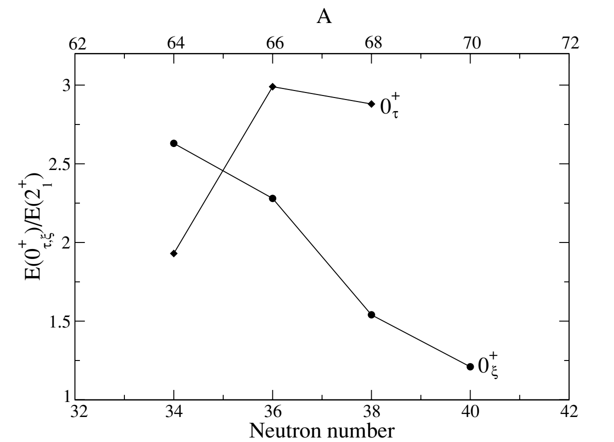

FIG. 9. Evolution of 0^+_ξ and 0^+_τ states in Zn isotopes, identified on the basis of the decay properties presented in Table II.

The geometric models fail in reproducing the trend of the experimental transition strengths in the ground state band of ^{64}Zn. The observed decrease of the strength with incresing spin could be due to the effect of the finite number of bosons (N_B).

Figure 8 (right) compares the same transition strengths with the prediction of the IBA limits U(5) and O(6) and with the critical point of the U(5)-O(6) transition, for $N_B = 4$. The results for the critical point of the U(5)-O(6) transition are obtained using the IBA Hamiltonian $H = \epsilon n_d + AP^\dagger P$, the critical point being defined, as given in ref. [5], by $\epsilon/A = 2(N_B - 1)$. The comparison shows that the IBA calculation at the critical point reproduces well the experimental transition strengths in the ground state band of ^{64}Zn. The disagreement between the geometric models and the IBA results are explained by the finite N_B effect [32], which is stronger for small N_B.

Other essential signatures of the E(5) symmetry are the decay properties of the first two 0^+ excited states labeled 0^+_ξ and 0^+_τ, which also vary along the U(5)-O(6) transition. 0^+_ξ evolves from a two-phonon state in U(5), with a strong $B(E2{:}0^+_\xi \rightarrow 2^+_1)$, into the $\sigma = \sigma_{\max} - 2$ state in O(6), which typically lies higher than the 4^+_1 and 2^+_1 states and the transition to the 2^+_1 state is forbidden. 0^+_τ is a member of the three-phonon multiplet all along the transition from U(5) to O(6), with a favored transition to the 2^+_2 state. In order to identify these states in ^{64}Zn, the behavior of the lowest excited 0^+ states in the Zn isotopic chain is studied qualitatively.

In Table II the decay properties of the 0^+ states in ^{64,66,68}Zn are given in comparison with the properties of the 0^+_ξ and 0^+_τ states predicted by the E(5) and O(5) symmetries. A behavior similar to that of the 0^+_τ state is observed for the 0^+_2 state in ^{64}Zn and the 0^+_3 states in ^{66,68}Zn. This behavior was observed also in Refs. [25,26]. Based on weak-coupling shell model calculations, Ref. [25] suggested that the 0^+_2 state in ^{64}Zn has a contribution from the intruder configuration $(1g_{9/2})^2_{J=0}$. Nevertheless, by analysing the transition strengths $B(E2{:}0^+_2 \rightarrow 2^+_2)/B(E2{:}2^+_1 \rightarrow 0^+_1) = 2.78(38)$ compared with the E(5) prediction of 1.92 and $B(E2{:}0^+_2 \rightarrow 2^+_1)/B(E2{:}2^+_1 \rightarrow 0^+_1) = 0.0026(3)$ compared with the E(5) prediction of 0.06, this state can be interpreted as the 0^+_τ predicted by the E(5) symmetry. Experimentally there is a E0 transition to the ground state reported by [26] with a relatively small transition strength of $\rho^2(0^+_2 \rightarrow 0^+_1) = 3.9(4) \times 10^{-3}$. This value is in disagreement with the E(5) symmetry where the transition strength E0: $0^+_\tau \rightarrow 0^+_1$ is zero. This disagreement was observed also for other E(5) nuclei like ^{134}Ba (with a $\rho^2(0^+_\tau \rightarrow 0^+_1) = 3.6(18) \times 10^{-3}$ [33]) and ^{102}Pd (with a $\rho^2(0^+_\tau \rightarrow 0^+_1) = 4.0(15) \times 10^{-3}$ [33]).

TABLE II. Decay properties of 0^+ states in ^{64,66,68}Zn.

	^{64}Zn	^{66}Zn	^{68}Zn	E(5)	O(5)	
$\frac{B(E2:0^+_2\rightarrow 2^+_2)}{B(E2:0^+_2\rightarrow 2^+_1)}$	1054	0.53	0	0.12	0	$\frac{B(E2:0^+_\xi\rightarrow 2^+_2)}{B(E2:0^+_\xi\rightarrow 2^+_1)}$
$\frac{B(E2:0^+_3\rightarrow 2^+_2)}{B(E2:0^+_3\rightarrow 2^+_1)}$	<0.66	210	>430	32	∞	$\frac{B(E2:0^+_\tau\rightarrow 2^+_2)}{B(E2:0^+_\tau\rightarrow 2^+_1)}$

Despite the disagreement in the level energy, the decay pattern of the 0^+_2 level is a strong argument for the identification of this state as the 0^+_τ state predicted by the E(5) symmetry.

The 0^+_3 state in ^{64}Zn and 0^+_2 states in ^{66,68}Zn show a behavior similar to that of the 0^+_ξ state predicted by the E(5) symmetry. The transitions strengths $B(E2{:}0^+_3 \rightarrow 2^+_1)/B(E2{:}2^+_1 \rightarrow 0^+_1) = 0.78(32)$ compared with the E(5) prediction of 0.49 and $B(E2{:}0^+_3 \rightarrow 2^+_2)/B(E2{:}2^+_1 \rightarrow 0^+_1) < 0.28$ compared with the E(5) prediction of 0.06 are solid arguments for the identification of the 0^+_3 state in ^{64}Zn as the 0^+_ξ state predicted by the E(5) symmetry.

With the above interpretation the evolution of the 0^+_ξ and 0^+_τ states in Zn isotopes is presented in Fig. 9.

IV. CONCLUSIONS

The staggering factor S_4 was used for the first time as a signature of the E(5) symmetry, along with the the $R_{4/2}$ ratio, in an extensive search for E(5) candidates. The best candidates in the Z, $N = 28$–50 were found to be ^{64}Zn, ^{68}Zn, and ^{64}Ge. Low-spin states in ^{64}Zn were populated in the ϵ/β^+ decay of ^{64}Ga and their properties were studied through γ-ray spectroscopy. The decay properties of the first two known excited 0^+ states were confirmed. The comparison with the predictions of the E(5) symmetry shows good agreement, including the decay of the 0_2^+ and 0_3^+ states, which can be considered as the 0_τ^+ and 0_ξ^+ states, respectively. The E(5) symmetry offers a new possible interpretation for the structure of the lowest excited 0^+ states in Zn isotopes.

ACKNOWLEDGMENTS

The authors acknowledge financial support from the CEEX program of the Romanian Ministry for Education and Research under Contract No. 05-D11-50.

[1] G. Scharff-Goldhaber and J. Weneser, Phys. Rev. **98**, 212 (1955).
[2] A. Bohr, Mat. Fys. Medd. K. Vidensk. Selsk. **26**, 14 (1952).
[3] L. Wilets and M. Jean, Phys. Rev. **102**, 788 (1956).
[4] F. Iachello and A. Arima, *The Interacting Boson Model* (Cambridge University Press, Cambridge, UK, 1987).
[5] A. E. L. Dieperink, O. Scholten, and F. Iachello, Phys. Rev. Lett. **44**, 1747 (1980).
[6] J. N. Ginocchio and M. W. Kirson, Phys. Rev. Lett. **44**, 1744 (1980).
[7] R. Gilmore, J. Math. Phys. **20**, 891 (1979).
[8] F. Iachello, Phys. Rev. Lett. **85**, 3580 (2000).
[9] F. Iachello, Phys. Rev. Lett. **87**, 052502 (2001).
[10] R. F. Casten and N. V. Zamfir, Phys. Rev. Lett. **85**, 3584 (2000).
[11] N. V. Zamfir *et al.*, Phys. Rev. C **65**, 044325 (2002).
[12] A. Frank, C. E. Alonso, and J. M. Arias, Phys. Rev. C **65**, 014301 (2002).
[13] R. M. Clark *et al.*, Phys. Rev. C **69**, 064322 (2004).
[14] J.-F. Zhang, G. Long, Y. Sun, S.-J. Zhu, F.-Y. Liu, and Y. Jia, Chin. Phys. Lett. **20**, 1231 (2003).
[15] N. V. Zamfir and R. F. Casten, Phys. Lett. **B260**, 265 (1991).
[16] B. Singh, Nucl. Data Sheets **78**, 395 (1996).
[17] J. Konjin, R. V. Lieshout, J. P. Deutsch, and L. Grenacs, Nucl. Phys. **A91**, 439 (1966).
[18] L. G. Mann, K. G. Tirsell, and S. D. Bloom, Nucl. Phys. **A97**, 425 (1967).
[19] S. Raman, N. B. Gove, and T. A. Walkiewicz, Nucl. Phys. **A254**, 131 (1975).
[20] ENSDF database, http://www.nndc.bnl.gov/ensdf/.
[21] R. F. Casten, in *Interacting Bose-Fermi Systems in Nuclei*, edited by F. Iachello (Plenum, New York, 1981).
[22] R. Bijker, R. F. Casten, N. V. Zamfir, and E. A. McCutchan, Phys. Rev. C **68**, 064304 (2003).
[23] E. A. McCutchan, N. V. Zamfir, and R. F. Casten, J. Phys. G **31**, S1485-S1490 (2005).
[24] F. Puelhofer, Nucl. Phys. **A280**, 267 (1977).
[25] A. Passoja, R. Julin, J. Kantele, J. Kumpulainen, M. Luotama, and W. Trzaska, Nucl. Phys. **A438**, 413 (1985).
[26] A. Passoja, J. Kantele, M. Luotama, J. Kumpulainen, R. Julin, P. O. Lipas, and P. Toivonen, Phys. Lett. **128B**, 157 (1983).
[27] D. N. Simister, L. P. Ekström, G. D. Jones, F. Kearns, T. P. Morrison, O. M. Mustaffa, H. G. Price, P. J. Twin, R. Wadsford, and N. J. Ward, J. Phys. G **6**, 81 (1980).
[28] J. M. Arias, Phys. Rev. C **63**, 034308 (2001).
[29] J. Leske, K. H. Speidel, S. Schielke, O. Kenn, D. Hohn, J. Gerber, and P. Maier-Komor, Phys. Rev. C **71**, 034303 (2005).
[30] R. B. Cakirli, R. F. Casten, J. Jolie, and N. Warr, Phys. Rev. C **70**, 047302 (2004).
[31] E. Williams *et al.*, Phys. Rev. C **74**, 024302 (2006).
[32] R. F. Casten and D. D. Warner, Rev. Mod. Phys. **60**, 389 (1988).
[33] T. Kibedi and R. H. Spear, At. Data Nucl. Data Tables **89**, 77 (2005).